Thermal properties of a two-dimensional intrinsically curved semiflexible biopolymer*

Zicong Zhou(周子聪)[1,†] and Yanting Wang(王延颋)[2,3]

[1] Department of Physics, Tamkang University, New Taipei City, Taiwan, China
[2] CAS Key Laboratory of Theoretical Physics, Institute of Theoretical Physics, Chinese Academy of Sciences, Beijing 100190, China
[3] School of Physical Sciences, University of Chinese Academy of Sciences, Beijing 100049, China

(Received 17 November 2016; revised manuscript received 9 December 2016; published online 18 January 2017)

We study the behaviors of mean end-to-end distance and specific heat of a two-dimensional intrinsically curved semiflexible biopolymer with a hard-core excluded volume interaction. We find the mean square end-to-end distance $R_N^2 \propto N^{\beta}$ at large N, with N being the number of monomers. Both β and proportional constant are dependent on the reduced bending rigidity κ and intrinsic curvature c. The larger the c, the smaller the proportional constant, and $1.5 \geq \beta \geq 1$. Up to a moderate $\kappa = \kappa_c$, or down to a moderate temperature $T = T_c$, $\beta = 1.5$, the same as that of a self-avoiding random walk, and the larger the intrinsic curvature, the smaller the κ_c. However, at a large κ or a low temperature, β is close to 1, and the conformation of the biopolymer can be more compact than that of a random walk. There is an intermediate regime with $1.5 > \beta > 1$ and the transition from $\beta = 1.5$ to $\beta = 1$ is smooth. The specific heat of the system increases smoothly with increasing κ or there is no peak in the specific heat. Therefore, a nonvanishing intrinsic curvature seriously affects the thermal properties of a semiflexible biopolymer, but there is no phase transition in the system.

Keywords: thermal property, semiflexible biopolymer, intrinsic curvature

PACS: 87.16.Ka, 87.15.hp, 87.15.ak, 87.15.Zg **DOI:** 10.1088/1674-1056/26/3/038701

1. Introduction

Temperature (T) seriously affects the property of a polymer. It is well known that a flexible polymer has three different phases below, at, or above the θ-temperature.[1] The θ-temperature is the temperature at which the phase transition takes place and it provides a clear border to separate these phases. At the θ-temperature, the excluded volume effect (EVE) can be ignored or the EVE is balanced by the attractive interactions between polymer segments and solvent molecules, the conformation of a polymer can be modeled as a random walk of monomer subunits, and such a polymer is referred to as an ideal chain, a free-jointed chain, or a Gaussian chain. Correspondingly, solvents at the θ-temperature are called θ-solvents.[1] Moreover, in good solvent or above the θ-temperature, EVE dominates the conformation of a polymer so that the chain is in a swollen state and can be described by a self-avoiding random walk (SAW).[1–7] In contrast, in poor solvent or below the θ-temperature, the attractive forces between different segments suppress the excluded volume effect so that the polymer chain collapses into a compact globule state. Temperature also greatly affects the mechanical property of a polymer. For swollen or ideal polymer chains, the polymer extends progressively with increasing force so that no sharp transition in extension occurs.[8–11] However, in poor solvent, the extension of a polymer is subjected to a first-order transition.[12–14]

Biopolymers can be classified as flexible and semiflexible. A flexible biopolymer means that to bend it does not cost any energy. It follows that its ground-state configuration (GSC, or the configuration with the lowest energy) is not unique so that there is no way to define an intrinsic curvature (IC), since a finite IC means that the GSC must have a well-defined curvature. However, many biopolymers, such as DNA, actin, and microfilament, are rigid or semiflexible. To bend these biopolymers locally subjects them to an energy penalty. The conformal and mechanical properties of semiflexible biopolymers have attracted lots of attention owing to their importance in understanding the structure and function of bio-materials. The simplest model for a semiflexible biopolymer is the wormlike chain (WLC) model and it describes well the entropic elasticity of an intrinsically straight semiflexible biopolymer.[15–18] The GSC of the WLC model is unique and is a straight line, and at finite T, a WLC extends gradually with increasing stretching force or there is no sharp transition in extension. However, intrinsically curved biopolymers are also ubiquitous. For instance, special sequence orders favor a finite IC for some short dsDNA chains.[19–22] It has also been reported that a long-range correlated dsDNA has a macroscopic (intrinsic) curvature so that the WLC model fails to account for its property.[23]

Recently, we found that a finite IC alone can induce a discontinuous transition in extension[24,25] for a two-dimensional (2D) long semiflexible biopolymer. The IC plays a similar

*Project supported by the Minister of Science and Technology of China
†Corresponding author. E-mail: zzhou@mail.tku.edu.tw

role as an attractive force in a poor solvent for a polymer and the bending rigidity plays the role of the strength of the attractive force. With a hard-core excluded volume interaction (EVI) and free of an external force, this system is the same as the SAW model if its bending rigidity is zero or at a very high temperature so the entropy dominates the conformation. On another limit, i.e., at a very large bending rigidity or at very low temperature, its conformation should be similar to an Archimedean spiral. The end-to-end distance of an Archimedean spiral is proportional to the square-root of its length. It is then intriguing to ask for such a system is there a temperature similar to the θ-temperature? In this work, we provide an answer to this question.

Moreover, recent progresses in experimental techniques make it possible to perform experiments on semiflexible biopolymers in a two-dimensional (2D) environment so that the property of biopolymers in 2D has attracted growing interest.[23–36] Therefore, for simplicity, we focus on the 2D system in this work.

The paper is organized as follows. In Section 2, we describe our model and simulation settings. In Section 3, we present the main results. The main text ends with conclusions and discussion.

2. Model and simulation settings

2.1. Model

A semiflexible biopolymer is often modeled as a filament. In a 2D case, the configuration of a filament is determined by a vector $\boldsymbol{t} \equiv \mathrm{d}\boldsymbol{r}/\mathrm{d}s = \{\cos\phi, \sin\phi\}$, which is tangent to the contour line of the filament, where $\boldsymbol{r} = (x, y)$ is the locus of the filament, s is the arc length, and $\phi(s)$ is the angle between the x-axis and $\boldsymbol{t}$, as shown in Fig. 1. One end of the chain (at $s = 0$) is fixed at $x = y = 0$, we can write the elastic energy of an external force-free intrinsically curved filament as[23,29,35]

$$E_L = \frac{k}{2}\int_0^L \mathrm{d}s(\dot{\phi} - \tilde{c})^2, \tag{1}$$

where k is the bending rigidity, L is the contour length as well as a constant so that the filament is inextensible, $\dot{\phi} \equiv \dot{x}\ddot{y} - \dot{y}\ddot{x}$ is the signed curvature, and $\tilde{c}$ is the intrinsic signed curvature. $\tilde{c} \neq 0$ means that the GSC of the filament is a curve of curvature $\tilde{c}$. The dot represents the derivative with respect to s. $\tilde{c}$ can be s-dependent, but for simplicity, in this work, we consider only an s-independent or constant $\tilde{c}$. $\tilde{c}$ can also be either positive or negative, but without loss of generality we assume $\tilde{c} > 0$.

Fig. 1. Schematic diagram of a filament showing the notation used.

The continuous model does not include the excluded volume interaction (EVI). However, it is unreasonable to ignore the EVI in a 2D system. To find an exact result is very difficult when we consider the EVI, so that we discretize the continuous model and perform Metropolis Monte Carlo simulation[6] to study it in the off-lattice system. In the discrete model, a filament consists of N straight segments of length l_0 joined end to end. The coordinates of the two ends of the i-th segment are therefore $\{x_{i-1}, y_{i-1}\}$ and $\{x_i, y_i\}$. By replacing $\dot{\phi}$ with $(\phi_{i+1} - \phi_i)/l_0$ and introducing the reduced energy, $\mathcal{E}_N \equiv E_N/k_\mathrm{B}T$, we can write

$$\mathcal{E}_N = \frac{\kappa}{2}\sum_{i=1}^{N-1}(\phi_{i+1} - \phi_i - c)^2 + \sum_{i<j} U_\mathrm{evi}(r_{ij}), \tag{2}$$

$$U_\mathrm{evi} = \begin{cases} \infty, & r_{ij} < l_0, \quad j \neq i \pm 1, \\ 0, & r_{ij} \geq l_0, \quad j \neq i \pm 1, \end{cases} \tag{3}$$

where k_B is the Boltzmann constant, T is the temperature, $c \equiv \tilde{c}l_0$, and $\kappa \equiv k/l_0 k_\mathrm{B}T = l_\mathrm{p}/2l_0$ is the reduced bending rigidity with l_p the 2D persistent length, so $T \propto 1/\kappa$, or with a fixed k, a larger κ gives a lower temperature. We also scale the length by l_0 so $x_N = x(L) = \sum_{i=1}^N \cos\phi_i$ and $y_N = y(L) = \sum_{i=1}^N \sin\phi_i$. U_evi is the simplest short range hardcore EVI, and $r_{ij} = |\boldsymbol{r}_i - \boldsymbol{r}_j|$ is the distance between the ends of i^th and j^th segments. When $\kappa = 0$, i.e., $k = 0$ or $T = \infty$, it becomes a 2D SAW chain with $R_N^2 \equiv R_L^2 \equiv \langle(\boldsymbol{r}_N - \boldsymbol{r}_0)^2\rangle = N^{2\nu}$ and $\nu = 0.75$.[1–7]

The thermal average, $\langle B\rangle$, of a physical quantity $B(\phi_1, \phi_2, \ldots, \phi_{N-1})$ is defined as the average with Boltzmann weight over all possible conformations, i.e.,

$$\langle B\rangle = \int\prod_{j=1}^{N-1}\mathrm{d}\phi_j B\exp(-\mathcal{E}_N)/\int\prod_{j=1}^{N-1}\mathrm{d}\phi_j\exp(-\mathcal{E}_N). \tag{4}$$

2.2. Simulation settings

In Metropolis Monte Carlo simulation, we equilibrate every sample from 10^6 to 2×10^6 Monte Carlo steps (MCS) before performing the averaging. The thermal average for a sample is taken from 2×10^7 to 3×10^7 MCS. Moreover, we take $N = 50$, 100, 200, 300, and 450 to examine the finite size effect. The range of κ is from 0 to 60. Note that the $l_\mathrm{p} = 2\kappa$ of a double-stranded DNA is about 50 nm. $c = 0.1$, 0.2, and 0.5. We do not consider a larger c because it is impractical. We use the hinged boundary condition (BC) in simulation, i.e., we do not fix ϕ_1 and ϕ_N.

The thermodynamical limit in this work means that we keep both l_0 and c as constants but let $N \to \infty$ so that the total length $L = Nl_0 \to \infty$. At a finite temperature, the fluctuation can suppress sharp transition, especially for a finite-size system. Therefore, to examine the occurrence of phase transition, one often has to evaluate the finite size effects. For this purpose, we evaluate the mean square end-to-end distance

R_N^2, mean energy $\varepsilon_N \equiv \varepsilon_L \equiv \langle \mathcal{E}_N/N \rangle$, and specific heat. From Eq. (4), we can calculate the specific heat from

$$S_N \equiv \frac{1}{N}\frac{\partial \langle E_L \rangle}{\partial T} = \frac{\partial \varepsilon_L}{\partial T} = \frac{k_B[\langle \mathcal{E}_N^2 \rangle - \langle \mathcal{E}_N \rangle^2]}{N}. \quad (5)$$

Exactly, in simulation we calculate $\mathcal{C}_N = S_N/k_B$. We also monitor $\langle x_N \rangle$, $\langle x_N^2 \rangle$, and $\langle y_N^2 \rangle$.

3. Results

The mechanical property of the model in absence of EVI has been studied.[24,25,35] It finds that a nonvanishing c can induce a discontinuous change in extension for a semiflexible biopolymer. At $T = 0$, the transition is multiple-step and accompanied by unwinding loops, regardless of κ and L. However, a finite temperature represses the transition so that the discontinuous transition becomes one-step, requires sufficient large c and κ, and probably occurs only in the thermodynamical limit. However, a full picture of the thermal property of the model is not yet available.

3.1. The $U_{evi} = 0$ case

When $U_{evi} = 0$, the R_L^2 has been found exactly as[35]

$$\begin{aligned} R_L^2 &= \frac{2l_pB}{(1+l_p^2\tilde{c}^2)^2}, \quad (6)\\ B &= L - l_p + l_p^2\tilde{c}^2 L + l_p^3\tilde{c}^2 \\ &\quad + \left[(l_p - l_p^3\tilde{c}^2)\cos(\tilde{c}L) - 2l_p^2\tilde{c}\sin(\tilde{c}L)\right] e^{-L/l_p}. \end{aligned}$$

Clearly R_L^2 is a continuous function of l_p or T. For a long chain ($L \gg l_p$), we find

$$R_L^2 \approx \frac{2l_pL}{1+l_p^2\tilde{c}^2} = \frac{4\kappa k_BTL}{k_B^2T^2 + 4\kappa^2\tilde{c}^2}. \quad (7)$$

It has a maximum value at $l_p = 1/\tilde{c}$ or $\kappa = 0.5/\tilde{c}$ with $R_L^2 = L/\tilde{c}$. With a fixed κ, when $T \to 0$ we obtain $R_L^2 = 2[1-\cos(\tilde{c}L)]/\tilde{c}^2$, so $R_L^2/L \to 0$, as it should be for the distance between two ends of an arc with radius of $1/\tilde{c}$. Meanwhile, $R_L^2/L \propto 1/\kappa$ at a large κ. On the other hand, $R_L^2/L \propto 1/T$ at a large T. When $\tilde{c} = 0$, it recovers the result of the WLC model except for when $T \to 0$ or $\kappa \to \infty$, since in this case $R_L^2 \to L^2$.

Because E_L is in a quadratic form when $\kappa > 0$, from the equipartition theorem, it is straightforward to know that $\varepsilon_L = k_BT/2$ and it follows $\mathcal{C}_L = 1/2$. In other words, both ε and $\mathcal{C}_L$ are independent of κ and $\tilde{c}$ when $\kappa > 0$. When $\kappa = 0$, $\langle E_L \rangle = 0$, so $\mathcal{C}_L = 0$. It means that $\kappa = 0$ is a singular point of $\mathcal{C}_L$. Since $\mathcal{C}_L$ is a constant when $\kappa > 0$, we conclude that there is no phase transition in the system when T varies, regardless of κ and $\tilde{c}$. The fact that R_L^2 is a continuous function of l_p or T further supports this conclusion. We should note that this conclusion is also valid for a 2D semiflexible biopolymer with short-range correlation in intrinsic curvatures, with a replacement of l_p by an effective persistent length.[36] This conclusion also suggests that the thermal property of the system is quite different from its mechanical property.

3.2. The $U_{evi} \neq 0$ case

3.2.1. End-to-end distance

At first, since we use a simple hard-core EVI, we expect that at a large κ or low T, the conformation of the system should tend to be close to an Archimedean spiral. In other words, the end-to-end distance of an Archimedean spiral gives a lower bound of R_L^2 of the current system. For an Archimedean spiral, $r(s) = a\theta(s)$, where θ is the polar angle in the plane polar coordinate system, and $\phi(s) = \theta(s) + \arccos(1/\sqrt{1+\theta^2(s)})$. It is also straightforward to show that for a long Archimedean spiral, $R_L^2/L \approx \sqrt{a}/2^{3/2}$ and the curvature at large s is close to zero. Since the EVI in Eq. (3) requires the shortest distance between any two parts of the filament to be 1, the corresponding Archimedean spiral has $a = 1/2\pi$ so $R_L^2/L \approx 1/4\sqrt{\pi}$. Such a spiral is much more compact than a random walk with $R_L^2/L \approx 1$, and is also very different from an intrinsically curved filament in the absence of EVI and with a R_L^2 given by Eq. (6).

Meanwhile, because we adopt the hinged BC, the system has a rotational invariance so that exactly $\langle x_N \rangle = 0$ and $\langle x_N^2 \rangle = \langle y_N^2 \rangle$ or $\alpha \equiv \langle x_N^2 \rangle / \langle y_N^2 \rangle = 1$. Our simulations agree with these results, and a typical example with $c = 0.5$ is presented in Fig. 2. Figure 2 also shows that the larger the N, the better the agreement.

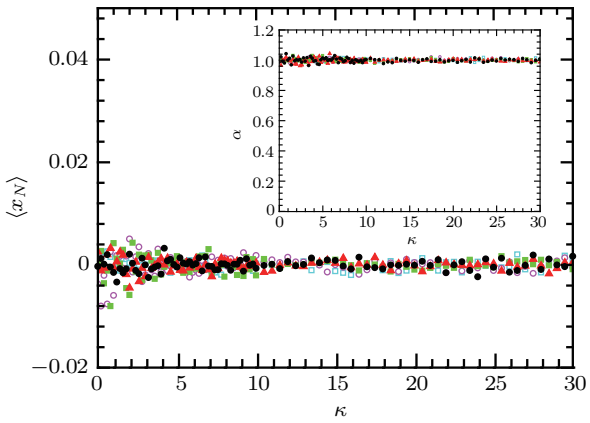

Fig. 2. (color online) $\langle x_N \rangle$ and $\alpha \equiv \langle x_N^2 \rangle / \langle y_N^2 \rangle$ (inset) vs. κ when $c = 0.5$ and $U_{evi} \neq 0$. $N = 50$ (cyan open square), 100 (magenta open circle), 200 (green solid square), 300 (red solid triangle), and 450 (black solid circle). The reduced units are used.

Moreover, from Figs. 3–5, we can see that when $\kappa = 0$ or $T = \infty$, the simulation gives $A \equiv R_N^2/N^{1.5} \approx 1$, and the larger the N, the better the approximation. This is a natural result since in this case the chain becomes a 2D SAW chain so $R_N^2 \approx N^{2\nu}$ with $\nu = 0.75$.[1–7] The above simulation results provide a robust proof on the correctness of the simulation.

From Figs. 3–5, we observe that at large N and up to a moderate $\kappa = \kappa_c$, all A's fall into the same curve for a given c. In other words, at large N it still satisfies $R_N^2 \approx AN^{1.5}$ up to

κ_c. A is almost independent of N, but is dependent on both κ and c, and the larger the c, the smaller the A, owing to that a large c favors a curled state. Figures 3–5 also show that A has a peak at $\kappa = \kappa^* < 0.5/c$, and the height of the peak decreases with increasing N and c. This tendency is similar to the system free of the EVI but with a smaller κ^*. At $c = 0.5$, the peak almost vanishes. Therefore, we conclude that the peak does not correspond to any phase transition. When $\kappa > \kappa^*$, A decreases with increasing κ, owing to that a large κ reduces the thermal effect so also favors a more curled state. Moreover, κ_c decreases with increasing c, because a larger c favors a more compact conformation. From Figs. 3–5 and 9, we can estimate that when $c = 0.1$, $\kappa_c \approx 14$; when $c = 0.2$, $\kappa_c \approx 9$; and when $c = 0.5$, $\kappa_c \approx 5$.

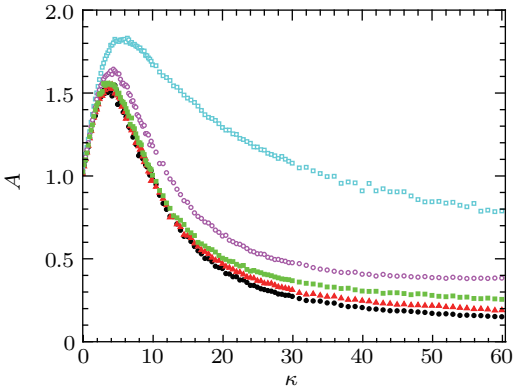

Fig. 3. (color online) $A \equiv R_N^2/N^{1.5}$ vs. κ when $c = 0.1$ and $U_{\rm evi} \neq 0$. The symbols are the same as those in Fig. 2. The reduced units are used.

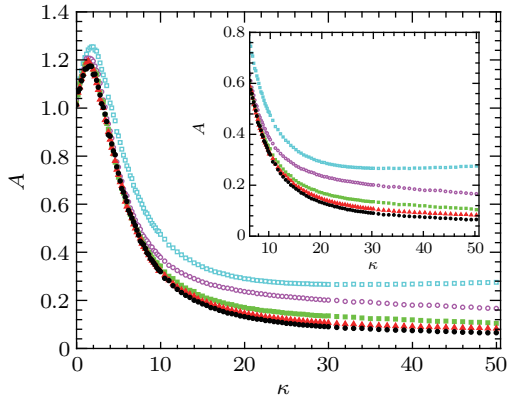

Fig. 4. (color online) A vs. κ when $c = 0.2$ and $U_{\rm evi} \neq 0$. The symbols are the same as those in Fig. 2. The inset is the blowup of the large κ regime. The reduced units are used.

However, also from Figs. 3–5, we find that when $\kappa > \kappa_c$, A no longer falls into the same curve at large N, and the larger the κ, the larger the visible discrepancy. Recall that at a large κ or low T, the conformation of the system should be similar to an Archimedean spiral which has $A' \equiv R_N^2/N \approx 1/4\sqrt{\pi}$ at large N, we evaluate A' and present the results in Figs. 6–8. From Figs. 6–8, we find that up to a rather large κ, A' increases clearly with increasing N so it indeed does not follow $R_N^2 \propto N$. But at a large $\kappa > \kappa_c'$, A' seems falling into the same curve again. We also note that in all cases, A' decreases with increasing κ, and can be smaller than 1 at large c, but is always larger than $1/4\sqrt{\pi}$, as shown in Fig. 8. It agrees with the conjecture that at a large κ or low T, the conformation of the system should tend to be close to an Archimedean spiral. But of course, it cannot be so compact as an Archimedean spiral so it must have $A' > 1/4\sqrt{\pi}$.

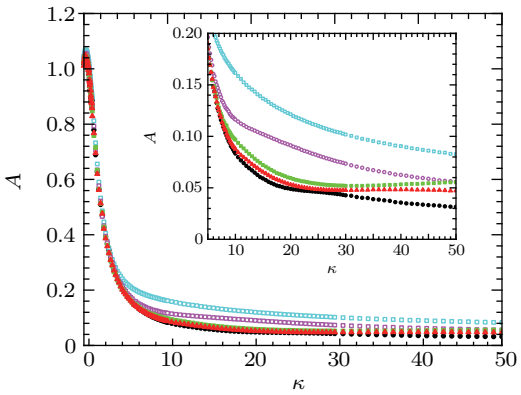

Fig. 5. (color online) A vs. κ when $c = 0.5$ and $U_{\rm evi} \neq 0$. The symbols are the same as those in Fig. 2. The inset is the blowup of the large κ regime. The reduced units are used.

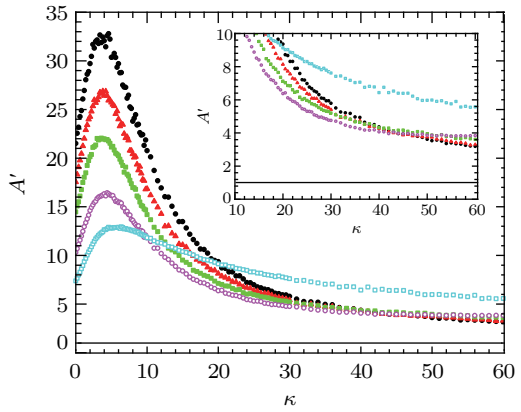

Fig. 6. (color online) A' vs. κ when $c = 0.1$ and $U_{\rm evi} \neq 0$. The black solid line is given by $A' = 1$. The other symbols are the same as those in Fig. 2. The reduced units are used.

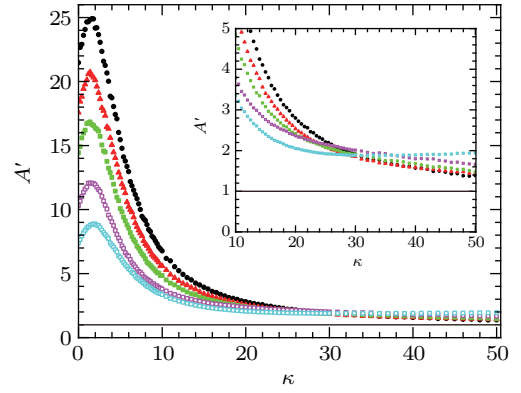

Fig. 7. (color online) A' vs. κ when $c = 0.2$ and $U_{\rm evi} \neq 0$. The black solid line is given by $A' = 1$. The other symbols are the same as those in Fig. 2. The reduced units are used.

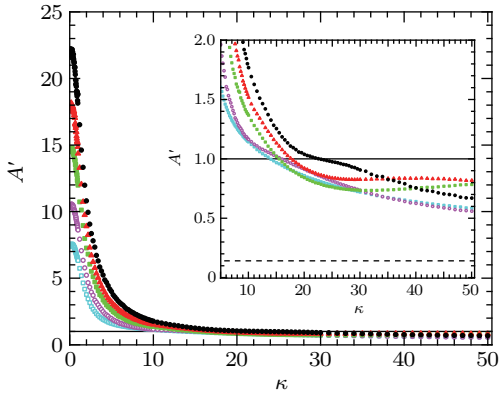

Fig. 8. (color online) A' vs. κ when $c = 0.5$ and $U_{\rm evi} \neq 0$. The black solid line is given by $A' = 1$. The black dashed line is given by $A' = 1/4\sqrt{\pi}$. The other symbols are the same as those in Fig. 2. The reduced units are used.

Furthermore, we calculate $\log R_N^2$ and fit it to $a_1 + \beta \log N$ using the data with $N = 100$, 200, 300, 450, as shown in Fig. 9. We discard the data with $N = 50$ because it obviously deviates from a straight line. β's have a large fluctuation because we have only 4 data points. However, from Fig. 9, we can find clearly that up to $\kappa \approx \kappa_c$, $\beta \approx 1.5$, and then β decreases almost linearly up to a moderate κ. But at a large κ ($> \kappa_c'$), β becomes flat again. From Fig. 9, we can see that $\kappa_c' \approx 50$, 40, and 30 when $c = 0.1$, 0.2, and 0.5, respectively. At large κ, β is close to 1 but can be smaller than 1, this should be due to N is not yet large enough. From Fig. 8, we also see that when $c = 0.5$, β is clearly larger than 1. It reflects the fact that a large c results in a large EVE, since a large c tends to bent the filament back to make a crossover.

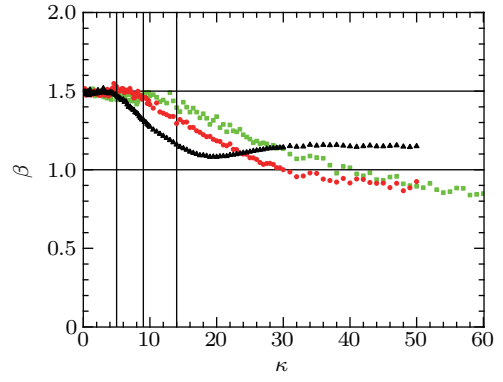

Fig. 9. (color online) β vs. κ when $c = 0.1$ (green solid square), $c = 0.2$ (red solid circle), and $c = 0.5$ (black solid triangle). Three vertical straight lines are given by $\kappa = 5$, 9, and 14. The reduced units are used.

From Figs. 3–9, we do not find any abrupt change in R_N^2. It follows that β goes smoothly from $\beta = 1.5$ to ≈ 1 with increasing κ or decreasing T. Recall that for flexible polymers in a dilute solvent, the θ-temperature is a phase transition temperature, so the behavior of R_N^2 or the value of β of the system has a discontinuous change at the θ-temperature, our results suggest that there is no phase transition in our system.

On the other hand, we do not find a compact globule state, i.e., a state with $\beta = 0.5$ like that found in the poor solvent for a flexible polymer.[7] This should be because we adopt a simple hard-core EVI which gives a lower bound of β, i.e., $\beta \geq 1$. However, we also find that it is possible to have $A' < 1$, i.e., to have a more compact conformation than a random walk. Therefore, a compact globule state is still possible if we adopt a relative soft-core EVI and it deserves a further investigation.

Finally, the elastic modulus under a uniaxial force can be found from[24,35]

$$\mu_N \equiv \frac{1}{N}\frac{\partial \langle x_N \rangle}{\partial f} = \frac{\langle x_N^2 \rangle - \langle x_N \rangle^2}{k_{\rm B}TN}, \tag{8}$$

where f is a uniaxial external force along x-axis. Since $\langle x_N \rangle = 0$ and $\langle x_N^2 \rangle = \langle y_N^2 \rangle$, we obtain $\mu_N = R_N^2/2N \propto N^{\beta-1}$ at large N.

3.2.2. Specific heat

When $\kappa = 0$, in this system we have exactly $\varepsilon_N = 0$ so that $\mathcal{C}_N = 0$, and our simulation confirms this result, as we can see from Figs. 10–12. Meanwhile, we find that $\mathcal{C}_N \approx 0.2\kappa$ up to $\kappa \approx 2$ for all c, as shown by the straight lines in Figs. 10–12. Comparing with that in the EVI-free system, we find that a nonvanishing EVI removes the singularity at $\kappa = 0$ for $\mathcal{C}_N$. Meanwhile, $\mathcal{C}_N$ is bounded at large κ, as shown in Figs. 10–12. The larger the c, the larger the upper limit of $\mathcal{C}_N$, and the upper limit is always larger than 0.5 which is the $\mathcal{C}_N$ of a system free of EVI. However, we should point out that we cannot fit $\mathcal{C}_N$ by either $\mathcal{C}_N \approx b_1(1 - {\rm e}^{-b_2\kappa})$ or $\mathcal{C}_N \approx b_1\kappa/(1 + b_2\kappa)$ for all κ with constant b_1 and b_2.

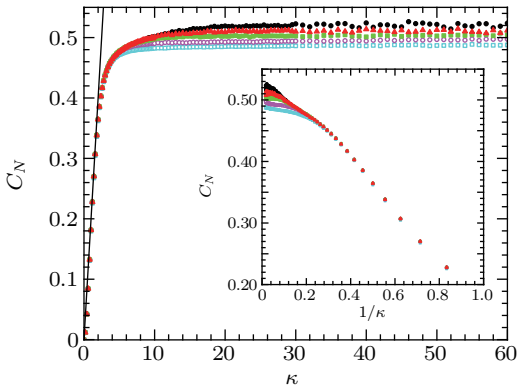

Fig. 10. (color online) $\mathcal{C}_N$ vs. κ ($1/\kappa$ in inset) when $c = 0.1$. The solid black line is given by $\mathcal{C}_N = 0.2\kappa$. The other symbols are the same as those in Fig. 2. The reduced units are used.

Finally, we do not find any clear peak in $\mathcal{C}_N$ in all cases, or $\mathcal{C}_N$ is a smooth function of κ or T. It therefore supports the conclusion obtained from R_N^2, i.e., there is not a unique κ or temperature, like the θ-temperature, to separate different states. At $c = 0.5$, we find that there exists an inflection point $\kappa = \kappa_i$ in which the curve of $\mathcal{C}_N$ vs. κ changes from being convex to concave, as shown in Fig. 12. In other words, when

$\kappa < \kappa_i$, $\mathcal{C}_N$ increases with acceleration with increasing κ; but when $\kappa > \kappa_i$, $\mathcal{C}_N$ increases with deceleration with increasing κ. However, this behavior is almost independent of N. Therefore, we conclude that no transition occurs in the system.

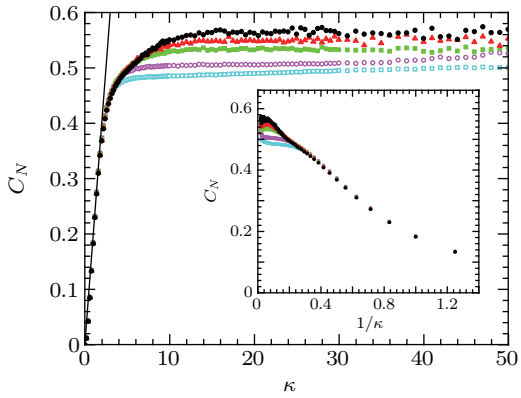

Fig. 11. (color online) $\mathcal{C}_N$ vs. κ ($1/\kappa$ in inset) when $c = 0.2$. The solid black line is given by $\mathcal{C}_N = 0.2\kappa$. The other symbols are the same as those in Fig. 2. The reduced units are used.

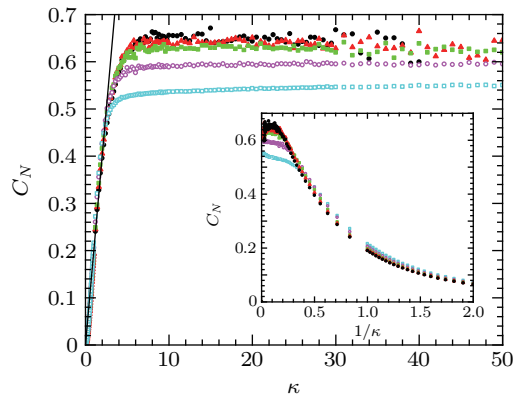

Fig. 12. (color online) $\mathcal{C}_N$ vs. κ ($1/\kappa$ in inset) when $c = 0.5$. The solid black line is given by $\mathcal{C}_N = 0.2\kappa$. The other symbols are the same as those in Fig. 2. The reduced units are used.

4. Conclusion

In summary, we study the thermal properties of a two-dimensional intrinsically curved semiflexible biopolymer with a simple hard-core EVI. We find that it always has $R_N^2 \approx AN^\beta$ at large N with A being an N-independent constant. However, both β and A are dependent on κ and c. A decreases with increasing c and $1.5 \geq \beta \geq 1$. Up to a moderate $\kappa = \kappa_c$, or down to a moderate temperature $T = T_c$, R_N^2 maintains the same behavior as a self-avoiding random walk, i.e., $\beta = 1.5$. The larger the c, the smaller the κ_c, owing to that a larger c favors a more compact state. However, at a large κ or a rather low temperature, β is close to 1, and the conformation can be more compact than that of a random walk since it can have $A < 1$. There is an intermediate regime with $1.5 > \beta > 1$ and the transition from $\beta = 1.5$ to $\beta = 1$ is smooth. Moreover, there is no peak in the specific heat or the specific heat is always finite. Therefore, we conclude that there is no phase transition in the system, but a nonvanishing intrinsic curvature still seriously affects the thermal property of the filament.

We focus on a constant intrinsic curvature in the present work, but we expect that the main conclusion is still valid for a 2D semiflexible biopolymer with short-range correlation in intrinsic curvatures. Moreover, we also expect that it is possible to observe similar phenomena in some constrained systems, such as in a flat box. We adopt a simple hard-core EVI in this work and it may prevent $\beta < 1$ so that a filament with a soft-core EVI deserves a further investigation.

References

[1] Doi M and Edwards S F 1986 *The Theory of Polymer Dynamics* (Oxford: Clearendon Press) p. 26
[2] Domb C 1963 *J. Chem. Phys.* **38** 2957
[3] McKenzie D S 1976 *Phys. Rep.* **27C** 35
[4] de Gennes P G 1979 *Scaling Concept in Polymer Physics* (Ithaca: Cornell UP)
[5] Essam J W 1980 *Rep. Prog. Phys.* **43** 833
[6] Landau D P and Binder K 2005 *A Guide to Monte Carlo Simulation in Statistical Physics* (2nd Edn.) (Cambridge: Cambridge University Press) pp. 78 and 85
[7] Bhattacharjee S M, Giacometti A and Maritan A 2013 *J. Phys.: Condens. Matter* **25** 503101
[8] Pincus P 1976 *Macromolecules* **9** 386
[9] Daoud M and de Gennes P G 1976 *J. Phys.* **38** 85
[10] Brochard-Wyart F 1993 *Europhys. Lett.* **23** 105
[11] Brochard-Wyart F, Hervet H and Pincus P 1994 *Europhys. Lett.* **26** 511
[12] Lai P Y 1995 *Physica A* **221** 233
[13] Lai P Y 1996 *Phys. Rev. E* **53** 3819
[14] Lai P Y 1998 *Phys. Rev. E* **58** 6222
[15] Marko J F and Siggia E D 1994 *Science* **265** 506
[16] Bustamante C, Marko J F, Siggia E D and Smith S 1994 *Science* **265** 1599
[17] Marko J F and Siggia E D 1995 *Macromolecules* **28** 8759
[18] Bouchiat C, Wang M D, Allemand J F, Strick T, Block S M and Croquette V 1999 *Biophys. J.* **76** 409
[19] Drew H R and Travers A A 1985 *J. Mol. Biol.* **186** 773
[20] Dlakic M, Park K, Griffith J D, Harvey S C and Harrington R E 1996 *J. Biol. Chem.* **271** 17911
[21] Han W, Lindsay S M, Dlakic M and Harrington R E 1997 *Nature* **386** 563
[22] Han W, Dlakic M, Zhu Y J, Lindsay S M and Harrington R E 1997 *Proc. Natl. Acad. Sci. USA* **94** 10565
[23] Moukhtar J, Fontaine E, Faivre-Moskalenko C and Arnéodo A 2007 *Phys. Rev. Lett.* **98** 178101
[24] Zhou Z, Lin F T, Hung C Y, Wu H Y and Chen B H 2014 *J. Phys. Soc. Jpn.* **83** 044802
[25] Zhou Z, Lin F T and Chen B H 2015 *Chin. Phys. B* **24** 028701
[26] Zhou Z and Joós B 2016 *Chin. Phys. B* **25** 088701
[27] Hernandez L I, Ramnarain S P, Huff E J and Wang Y K 1993 *Science* **262** 110
[28] Arnéodo A, Bacry E, Graves P V and Muzy J F 1995 *Phys. Rev. Lett.* **74** 3293
[29] Vaillant C, Audit B and Arnéodo A 2005 *Phys. Rev. Lett.* **95** 068101
[30] Maier B, Seifert U and Radler J O 2002 *Europhys. Lett.* **60** 622
[31] Marenduzzo D, Maritan A, Rosa A and Seno F 2003 *Phys. Rev. Lett.* **90** 088301
[32] Rosa A, Marenduzzo D, Maritan A and Seno F 2003 *Phys. Rev. E* **67** 041802
[33] Prasad A, Hori Y and Kondev J 2005 *Phys. Rev. E* **72** 041918
[34] Kulić I M, Mohrbach H, Thaokar R and Schiessel H 2007 *Phys. Rev. E* **75** 011913
[35] Zhou Z 2007 *Phys. Rev. E* **76** 061913
[36] Zhou Z and Joós B 2009 *Phys. Rev. E* **80** 061911